"EVALUATING AND COMPARING BONY DEFECTS ON HUMAN DRY MANDIBLES WITH CBCT IMAGES AND 3D PRINTED MODELS – AN IN VITRO STUDY."

By

REG NO. IG0221001

Dissertation

Submitted to KLE Academy of Higher Education and Research (KAHER), Belagavi
in Partial Fulfillment of the Requirements for the Degree Of

MASTER OF DENTAL SURGERY

In

ORAL MEDICINE AND RADIOLOGY

(BRANCH- VII)

DEPARTMENT OF ORAL MEDICINE AND RADIOLOGY

KAHER'S KLE VISHWANATH KATTI

INSTITUTE OF DENTAL SCIENCES, JNMC CAMPUS

NEHRU NAGAR, BELAGAVI- 590010, KARNATAKA.

2021 - 2024

KLE Academy of Higher Education and Research, Belagavi, Karnataka.

ENDORSEMENT BY THE HOD, PRINCIPAL/ HEAD OF THE INSTITUTION

This is to certify that this dissertation/ thesis entitled ***"Evaluating and comparing bony defects on human dry mandibles with CBCT images and 3D printed models – An in vitro study"***- is a bonafide research work done by **Reg: IG0221001**

HOD Keluskar

Dr. VAISHALI KELUSKAR, M.D.S.,
Professor and Head,
Department of Oral Medicine and Radiology
KLE Vishwanath Katti Institute of Dental Sciences, JNMC Campus, Nehru Nagar, Belagavi-590010.

Date: 20-4-2024
Place: Belagavi

Professor and Head
Department of Oral Medicine and Radiology
KLE VK Institute of Dental Sciences, Belagavi

Principal

Dr. ALKA D KALE, M.D.S., Ph.D.,
Principal,
KLE Vishwanath Katti Institute of Dental Sciences, JNMC Campus,
Nehru Nagar, Belagavi- 590010

Date: 20/4/24
Place: Belagavi

PRINCIPAL
KLE V.K. Institute of Dental Sciences
Nehru Nagar BELAGAVI-590010

LIST OF ABBREVIATIONS

ABBREVIATION	FULL FORM
CT	Computed Tomography
MSCT	Multi-slice spiral CT
CBCT	Cone Beam Computed Tomography
2D	Two Dimension
3D	Three Dimension
TMJ	Tempero mandibular joint
DICOM	Digital Imaging and Communications in Medicine
STL	Standard Tessellation Language
SLA	Stereolithography
DLP	Digital light processing
FFF	Fused filament fabrication
FDM	Fused deposition modeling
PSP	Photostimulable phosphor
CMOS	Complementary metal-oxide-semiconductor sensors
UV	Ultraviolet
SPSS	Statistical Package for the Social Sciences
ANOVA	Analysis of Variance
FOV	Field of view
kVp	Kilovoltage peak
mAs	Milliampere-seconds
mm	Millimeter
cm	Centimeter
h	Height
W	Width
OPG	Orthopantomogram

ABSTRACT

BACKGROUND:

A cone beam computed tomography (CBCT) has proven to be an effective tool in dental diagnosis and treatment planning due to its accuracy and reliability. The 3D printing process creates objects one layer at a time by adding layers. A more accurate, customized, and effective approach to healthcare is provided by the combination of CBCT and 3D printing, which improves treatment results and patient satisfaction.

AIM:

To evaluate the accuracy of CBCT images and 3D-printed models acquired by CBCT imaging.

MATERIALS AND METHODS:

By using cylindrical burs, bilateral circumferential bone defects were created on 10 dry human mandibles on symphysis and parasymphysis regions. Later, CBCT scans were performed on dry mandibles. The scanned images were exported in DICOM format and then converted into STL files, which are used as a format for 3D printing. The measurements were done using the Sidexis tool on CBCT, using a digital vernier caliper on dry mandibles and 3D models, followed by a statistical analysis of the data.

RESULTS:

A statistically insignificant difference ($p>0.05$) was found between dry mandibles and their CBCT images, similarly between CBCT and 3D printed models. However, the measurements

on the circumferential bony defects on the ramus of dry mandible models and 3D printed models were significantly different in width on the right and left sides (p =0.005 and 0.010), and in height on the left (p =0.033). Additionally, a significant difference (p =0.005) was found between the dry mandible and the 3D-printed model on the right side of parasymphysis.

CONCLUSION:

It was found that the accuracy of models derived from CBCT images was only slightly different. Thus, it has a variety of clinical applications in dentistry.

KEYWORDS: Cone-Beam Computed Tomography; Printing, Three-Dimensional; Models, Anatomic.

CONTENTS

LIST OF TABLES

LIST OF GRAPHS

LIST OF FIGURES

LIST OF ANNEXURES

INTRODUCTION

INTRODUCTION

It has been a boon to mankind, especially for health sciences since Wilhelm Roentgen discovered X-rays in 1895. Radiology has facilitated diagnosis and treatment planning and this field has seen tremendous progress over the years, especially in the last century [1]. Conventional radiographs like intraoral or panoramic radiographs, give a 2-dimensional image hence it does not provide accurate information for comprehensive preoperative planning surgeries and other procedures. To overcome this limitation of conventional radiography, various specialized radiographic techniques have been introduced in the recent past like cross-sectional tomograms, CT scans, and, more recently, cone beam CT (CBCT) which gives a precise diagnosis [2].

The introduction of computed tomography (CT) by Godfrey Hounsfield in 1972 revolutionized radiography as this allowed visualization of normal and abnormal soft tissue and bony structures [3]. Though CT offers various advantages over conventional radiography, it still has its drawbacks like high radiation dose, cost factor, poor resolution, etc in dentistry, its use is limited.

The advent of CBCT in 1982, has helped to overcome the limitations of CT, as this technique uses fan beam or spiral scans, specifically designed for imaging the maxillofacial region. This marks a new era in Radiology, as it enables a faster capture of all data from the entire field of view (FOV) by using a cone beam projector and a comparatively low radiation dose [3]. The advantage of CBCT over CT is the use of cone-shaped beam and solid-state flat panel detector, involving a 180-360 degree rotation around patient, thus imaging a specific area which could be the entire

dental/maxillofacial region or a single tooth [4]. The other advantages of CBCT include producing 3D images of actual size, with no distortions or overlaps [5]. The radiation dose is also minimal as compared to spiral CT [6]. The biggest advantage is the rapid scanning time which improves patient compliance [7]. The other applications of CBCT in Dentistry include diagnosis of unerupted and supernumerary teeth [8], assessing the upper airway volumes in 3D [9], analysis for orthognathic and orthodontic treatment planning [10], pre- and post-implant assessment, evaluating facial trauma, and fibro-osseous lesions within the TMJ [7]. As imaging technology has progressed over the last few years, the advent of 3D printing has led to an industrial revolution where raw materials can be converted into a model [11]. 3D-images can be generated by CBCT scans in either format or proprietary format. A specialized software package converts DICOM data to Standard triangular language files that represent a virtual 3D surface shape [12]. The applications of 3D models in Dentistry are in identifying anatomical landmarks, diagnosis and treatment planning, communication, vital role in image-guided surgeries, and prosthesis fabrication [13]. There are various methods for printing 3D objects, including inkjet printing, binder jet printing, fused deposition, laser sintering, stereolithography, and pressure-assisted micro syringe printing [14]. The most common techniques include: digital light processing, material jetting, and fused filament fabrication [15]. Binder/powder materials, which include polymers like resins and thermoplastics, ceramics, and metals are the main raw materials that are used in 3D printing, especially for applications in Dentistry [16].

Similarly in the current study, we have evaluated the dimensional accuracy of anatomical landmarks and artificially created circumferential bone defects on the human dry mandibles using CBCT scans and 3D printed model, respectively.

HYPOTHESIS

HYPOTHESIS

Null hypothesis:

There will be no dimensional changes in artificially created bone defects and anatomical landmarks of dry mandibles when compared with CBCT scans and 3D printed models.

Alternative hypothesis:

There will be dimensional changes in artificially created bone defects and anatomical landmarks of dry mandibles when compared with CBCT scans and 3D printed models.

AIM AND OBJECTIVES

Aim of the study:

The aim of this study was to evaluate and compare the dimensional accuracy of defects on dry mandibles, CBCT images of dry mandibles, and 3D-printed models.

Objectives:

1. To evaluate the dimensions of anatomical landmarks and artificially created circumferential bone defects in dry mandibles.
2. To evaluate the dimensions of anatomical landmarks and artificially created circumferential bone defects in CBCT scans.
3. To evaluate the dimensions of anatomical landmarks and artificially created circumferential bone defects in 3D printed models.
4. To compare the dimensions of anatomical landmarks and artificially created circumferential bone defects of the dry mandible, CBCT scans and 3D printed models.

REVIEW OF LITERATURE:

A dental x-ray is an essential diagnostic tool, used for diagnosis, treatment planning, and post-treatment evaluation of the patient [17][18].

Dental Radiographs:

There has been significant progress in dental radiography, including a study conducted by Franklin W. McCormack that examined the application of paralleling techniques in intraoral dental radiography [19]. Sialography, which was invented in 1925, is a form of radiography, that helps to evaluate several types of pathosis including tumours, duct obstructions, and inflammatory disorders, such as Sjögren's syndrome [20]. In 1960, the invention of Orthopantomography by Paatero revolutionized radiology and this was widely used in clinical practice [21]. An intra-oral detector based on digital charge-coupled devices (CCDs) was introduced in 1987. Even though the spatial resolution of the image was lower than that of the film, the advantages of having the image instantly available and reducing patient exposure were evident [22]. Photostimulable phosphor (PSP) receptors were introduced in 1994 [23]. A complementary metal-oxide-semiconductor sensor was first commercialized in 1998 [22]. All these advancements have a limitation of superimposition due to overlapping structures and improper detailing of the 3-dimensional volume of the human body that is represented as the 2-dimensional images.

Three-dimensional radiographs:

Computed tomography (CT) was introduced in 1967 by Godfrey N. Hounsfield where X-ray measurements of a body were taken from different directions which allowed the reconstruction of the internal structure [24]. The use of CT scans can be directed at

identifying pathologic processes, displaying trauma, assessing the paranasal sinuses, and investigating the temporomandibular joint bone to determine the best places for pre-surgical implant placement [25].

Although CT geometrics has progressed from parallel beam geometry to helical geometry, due to high radiation doses, high costs, lack of availability, longer scanning times, poor resolution, and difficulty in interpretation, CT has been limited in dentistry.

CBCT developed in the 1990s as a result of the increasing demand for three-dimensional images provided by conventional CT scans [26].

Cone beams generate more focused beams with considerably less radiation scattering [27]. CBCT technology is commonly used in the head and neck for evaluating impacted teeth, planning implants, evaluating the temporomandibular joint (TMJ), preparing orthodontics and surgical procedures, analysing dentoalveolar pathology, evaluating nasal/paranasal sinuses, pharyngeal airways, and providing information for rapid prototyping of 3D models [28].

3- Dimensional printing:

In three-dimensional printing or rapid prototyping, materials are combined through the application of computer-aided design to produce a customized three-dimensional object by selecting, depositing, or consolidating successive layers of material by selectively curing and deposition [29].

The first 3D printing process to be commercially available was invented by Charles Hull in 1980, which was the first 3D printing system to be patented [30]. Various 3D printing techniques have been developed based on various working concepts, such as: Inkjet

Printing, Binder Jet Printing, Fused Deposition Modelling, Selective Laser Sintering, and Stereolithography. [31].

3D - Printing in Dentistry:

Volumetric data can be used to generate 3D prints, allowing healthcare professionals to create dental models for presurgical planning or patient education, surgical templates, identification of anatomic landmarks i.e, mental plexus and dental devices for improving quality of life.

LITERATURE SEARCH:

CBCT and human dry mandible:

Kamburolu et al in **2011**, compared the CBCT measurements with direct digital callipers measurements of a human dry skull. It showed high correlations; for the first and second readings, they ranged from 0.992 to 1, respectively. A high correlation was found between measurements taken with digital callipers and CBCT [32].

Carolina et al in **2016**, scanned 12 dried human mandibles with various voxel sizes to generate CBCT images. There was high precision for all CBCT images, except for measurements using 0.4-mm voxels for mandibular incisors [33].

Fernandes et al in **2014,** observed that CBCT multiplanar reconstruction measurements exhibit extremely high interobserver reliability, with ICCs ranging from 0.63 to 0.99 and absolute measurements between the first and second measurements varying from 0 to 2.12mm [34].

CT and human dry mandible:

Jung et al in **2002,** obtained MDCT images of dry human skulls at various slice thicknesses and acquisition modes. It was found that all scan modes had no significant impact on distance-measuring accuracy. However, Smaller acquisition slice thicknesses resulted in better accuracy for each scan mode [35].

Measurements on human dry mandible from CBCT and CT:

Loubele et al in **2007**, noted that the direct measurements of the mandible showed a difference of 0.23 mm and 0.34 mm, as compared with CBCT and spiral tomography. In terms of vision and ability to distinguish periodontal tissues, the CBCT had a marked advantage over the MSCT [36].

Silva et al in **2017,** reported that both CBCT and MSCT software packages calculated anatomic distances accurately compared to digital callipers measurements of ten mandibles, which were not statistically significant ($p>0.05$) [37].

CBCT and 3D-printed model:

Raphael Olszewski et al in **2021** compared a dry human mandible to its corresponding 3D-model to determine the accuracy of a low-cost paper-based 3D-printer. The absolute mean difference was 0.36 ± 0.29 mm, while the relative difference was 1.87 ± 3.14%" [38].

Ruben R. Santana in **2012**, compared the measurements from CBCT images to STL models of twelve human mandibles. There was a mean difference of 0.35mm between CBCT and STL ($P = .048$) [39].

Poleti et al in **2021**, evaluated the linear measurements taken directly on the mandibles and 3D models obtained from CBCT. They concluded that an underestimation of 1mm

was noted for measurements carried out in 3D models. Also, inter-observer reliability was found to be greater than 0.75 for all the measured variables [40].

Joshua M. Ferraro in **2022**, found a significant difference between three-dimensional printed models of mandibular teeth made from intraoral scanners (IOS) and CBCT [41].

Xiaotong Wang in **2023**, found that the high and medium-cost jetting models had similar overall dimensional errors (0.07 ± 0.01 mm and 0.07 ± 0.03 mm), indicating their suitability for clinical applications like pre-bending plates and implant fabrication [42].

CT and 3D-printed model:

Ibrahim et al in **2009**, revealed that the SLS models (dimension error = 1.79%) and dry mandibles (dimensional error = 3.14%) were found to be the closest, followed by Poly Jet^{TM} and 3DPTM models (2.14% and 3.14%, respectively) [43].

CBCT and CT-derived 3D-printed model:

Yousefi et al in **2021,** observed that the measurements of both the FDM and DLP prototypes obtained from CBCT with small-FOV and large-FOV scanners showed no significant difference in dimensions of <0.7mm and 2.2mm respectively [44].

B.T. Primo in **2012** observed that the prototype produced from MSCT data showed a mean dimensional error of 0.62%, whereas CBCT images showed errors of 0.74%and 0.82% [45].

METHODOLOGY

STUDY DESIGN:

The current study is an in vitro study, to evaluate the dimensional accuracy of artificially created defects on 10 dry human mandibles and compare it with CBCT scans of dry mandibles and 3D-printed models with the same defects. This study was conducted based on the ethical standards set by the Declaration of Helsinki, including all amendments and revisions.

SOURCE OF DATA:

1. Human dry mandibles were collected from the Department of Forensic Medicine and Toxicology, Jawaharlal Nehru Medical College and Hospital, Belagavi, Karnataka.
2. CBCT scans of the dry mandibles were obtained from the Department of Oral Medicine and Radiology, KLE VK Institute of Dental Sciences, KLE Academy of Higher Education and Research (KAHER), Belagavi.
3. 3D models were printed from the Department of Mechanical Engineering and Technology, KLE DR.M Sheshagiri College of Engineering and Technology.

SELECTION CRITERIA:

Inclusion criteria:

1. Human dry adult mandibles.
2. Dry mandibles without any metal fillings.
3. Dry mandibles without any crowns or bridges.
4. Preserved mandibular bone cortices.

Exclusion criteria:

1. Mandible with anatomical deformity.
2. Fractured mandible.
3. Mandible with titanium miniplate, metal fillings, and dental prosthesis.

ARMAMENTARIUM:

1. Human Dry Mandibles (Figure 1)
2. Cylindrical bur-No:8,10 (Figure 2)
3. Digital vernier callipers (Figure 3)
4. High-rotation micromotor.
5. Dentsply Sirona Axeos CBCT machine (Figure 4)
6. Sidexis CBCT viewing software (version 4.3.1.0)
7. Exposure parameter (Figure 5)
8. Measuring tool (Figure 6)
9. SLA printer- form 2 printer (Figure 7)
10. Slicer 3D software
11. Scoring sheet for recording the observations.

METHOD:

A total of ten dry human mandibles were used for the study where four standardized circumferential bone defects were created using cylindrical burs numbers 10 and 8, under focused light of the dental equipment. Two defects were made on the ramus of the

mandible bilaterally (Figure 8) and the other two were made in the para symphysis region (Figure 9).

Linear measurements (height and width) of artificially created bone defects and anatomical landmarks on dry mandibles were measured with the help of digital vernier callipers.

A customized mount was made with the help of a cylindrical plastic container with a lid, which had a provision to place modelling clay or medium body silicone putty, over which the mandible could be placed before imaging. A cylindrical plastic container or plastic sheet was wrapped around the mounted mandible, to simulate the soft tissue.

CBCT scans were made of these dry mandibles with anatomical landmarks and artificially created bone defects using CBCT (Dentsply Sirona Axeos). The reference point was adjusted so that the midline corresponds to the junction of mandibular central incisors. The exposure parameters were set at 85kVp,12mA, scanning time of 14.8 seconds, and field of view (FOV) of 11*10 cm^2 for imaging. The anatomical landmarks and bone defects were measured in sagittal sections and then entered in an Excel sheet. The scanned images were subsequently exported to DICOM (Digital Imaging and Communications in Medicine) format. The DICOM format was converted into STL (Standard Tessellation Language) files using Slicer 3D software to create the 3D printed model. 3D printing of the scanned model's STL file was done using SLA additive manufacturing techniques. The model was printed using the Form 2 printer (Figure 7) and grey photopolymer resin (Acrylonitrile Butadiene Styrene "ABS" resin). The anatomical landmarks and artificially created bone defects were then measured on 3-D printed models with the help of digital vernier callipers. The measurements were repeated by the second observer. The measurements thus obtained from the dry

mandible, CBCT scans, and 3D printed models were statistically analysed using descriptive statistics analysis.

Measurement of parameters:

Fourteen linear measurements (Figure 10-16), were obtained in (mm) using a digital calliper with a (0-150) mm measuring range.

1. Length of the Right Ramus (Figure 10).
2. Length of the Left Ramus.
3. Height of the circumferential defect in the right ramus (Figure 11)
4. Height of the circumferential defect in the left ramus.
5. Width of the circumferential defect in the right ramus (Figure 12)
6. Width of the circumferential defect in the left ramus.
7. Height of the circumferential defect in the right Para symphysis (Figure 13)
8. Height of the circumferential defect in the Left Para symphysis.
9. Width of the circumferential defect in the right Para symphysis (Figure 14)
10. Width of the circumferential defect in the left Para symphysis.
11. Distance from the right circumferential defect in the ramus to the mental foramen (Figure 15)
12. Distance from the left circumferential defect in the ramus to the mental foramen.
13. Distance from the right circumferential defect in Para symphysis to the mental foramen (Figure 16).

14. Distance from left circumferential defect in Para symphysis to the mental foramen.

STATISTICAL ANALYSIS:

The data was entered in Microsoft Excel and statistically analysed using the SPSS software, version 21; SPSS Inc., (Chicago, IL, USA). The normality of the data was assessed prior to analysis using the Shapiro-Wilk's test/Kolmogorov-Smirnov test. Data was found to be normally distributed. Thus, the parametric test was chosen. Descriptive statistics was used to calculate frequencies, mean, and standard deviation values. Accordingly, One-way ANOVA followed by post hoc Tukey tests were carried out to determine the difference between various parameters. All statistical tests were performed at a significance level of 5% ($p < 0.05$).

PHOTOGRAPHS

Figure 1: Human dry mandible

Figure 2: Cylindrical bur

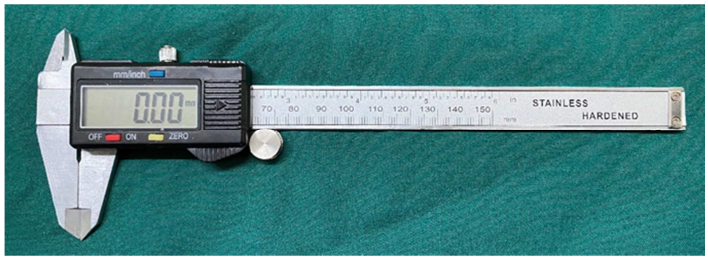

Figure 3: Digital vernier caliper.

Figure 4: Dentsply Sirona Axeos CBCT machine

Figure 5: Exposure Parameter

Figure 6: Measuring Tools

Figure 7: 3D Printer

Figure 8: Artificially created circumferential defect on the Mandibular ramus.

Figure 9: Artificially created circumferential defect on the Mandibular para symphysis.

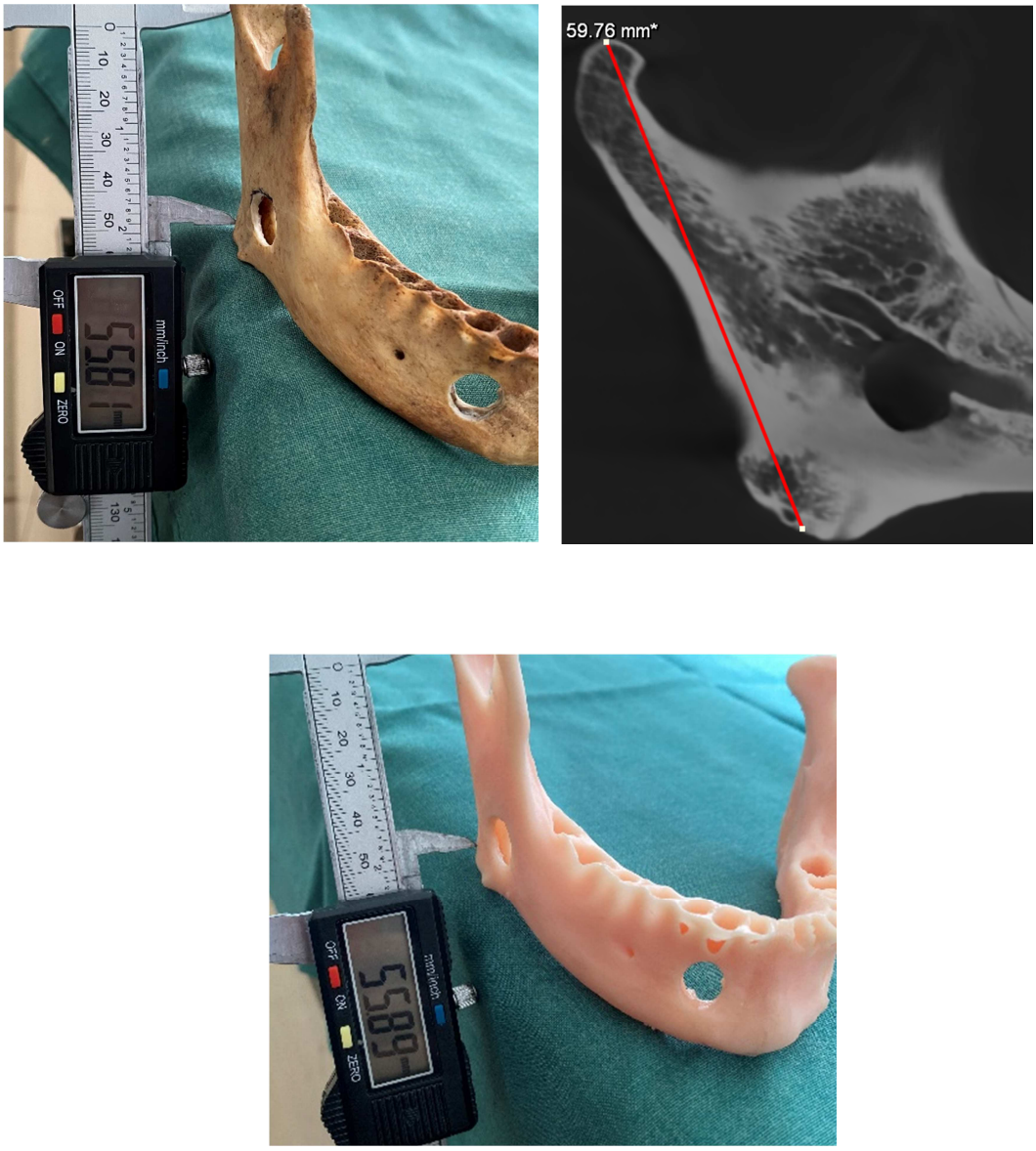

Figure 10: Measurement of length of mandible.

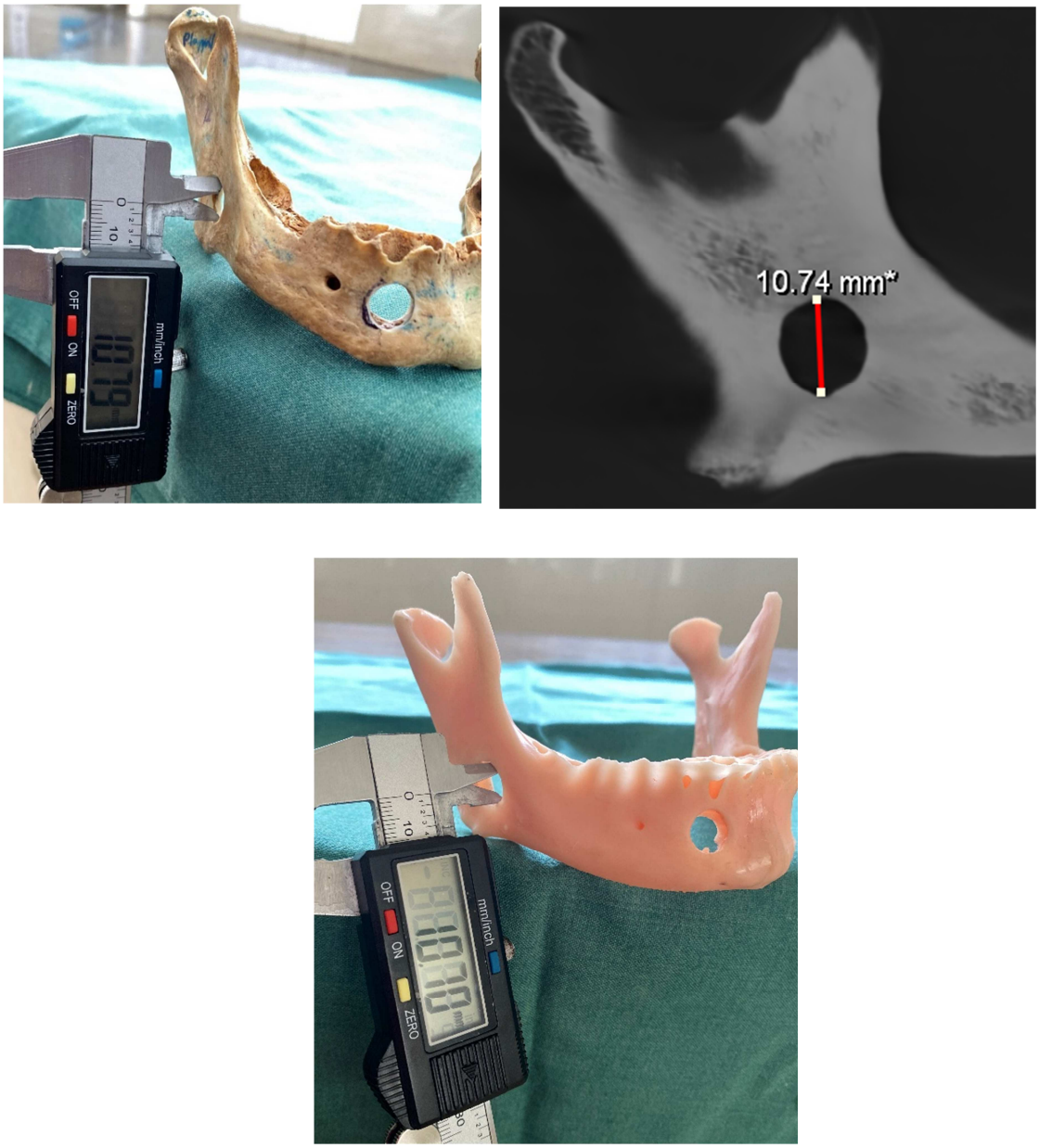

Figure 11: Measurement of circumferential defect height in ramus.

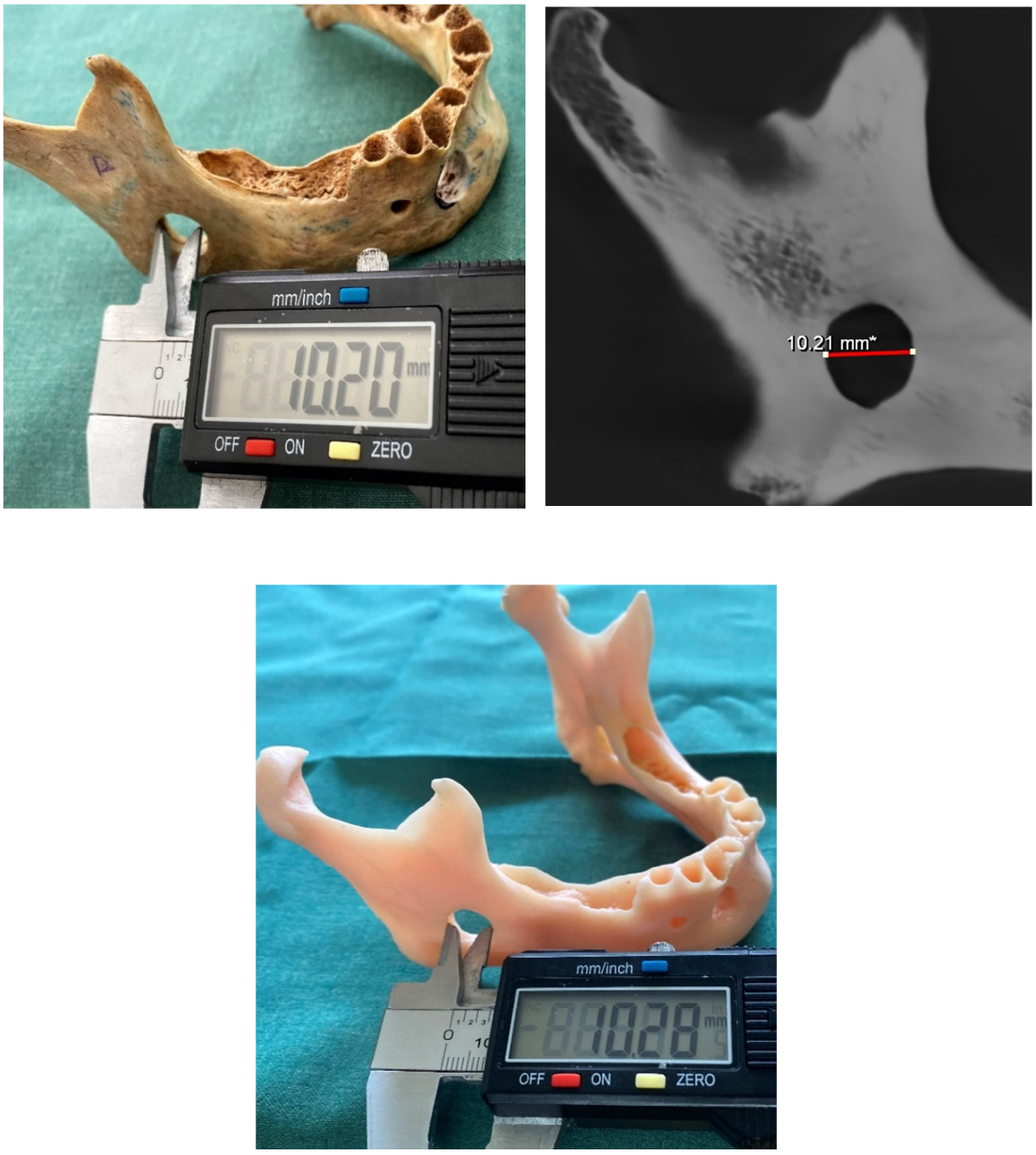

Figure 12: Measurement of circumferential defect width in ramus.

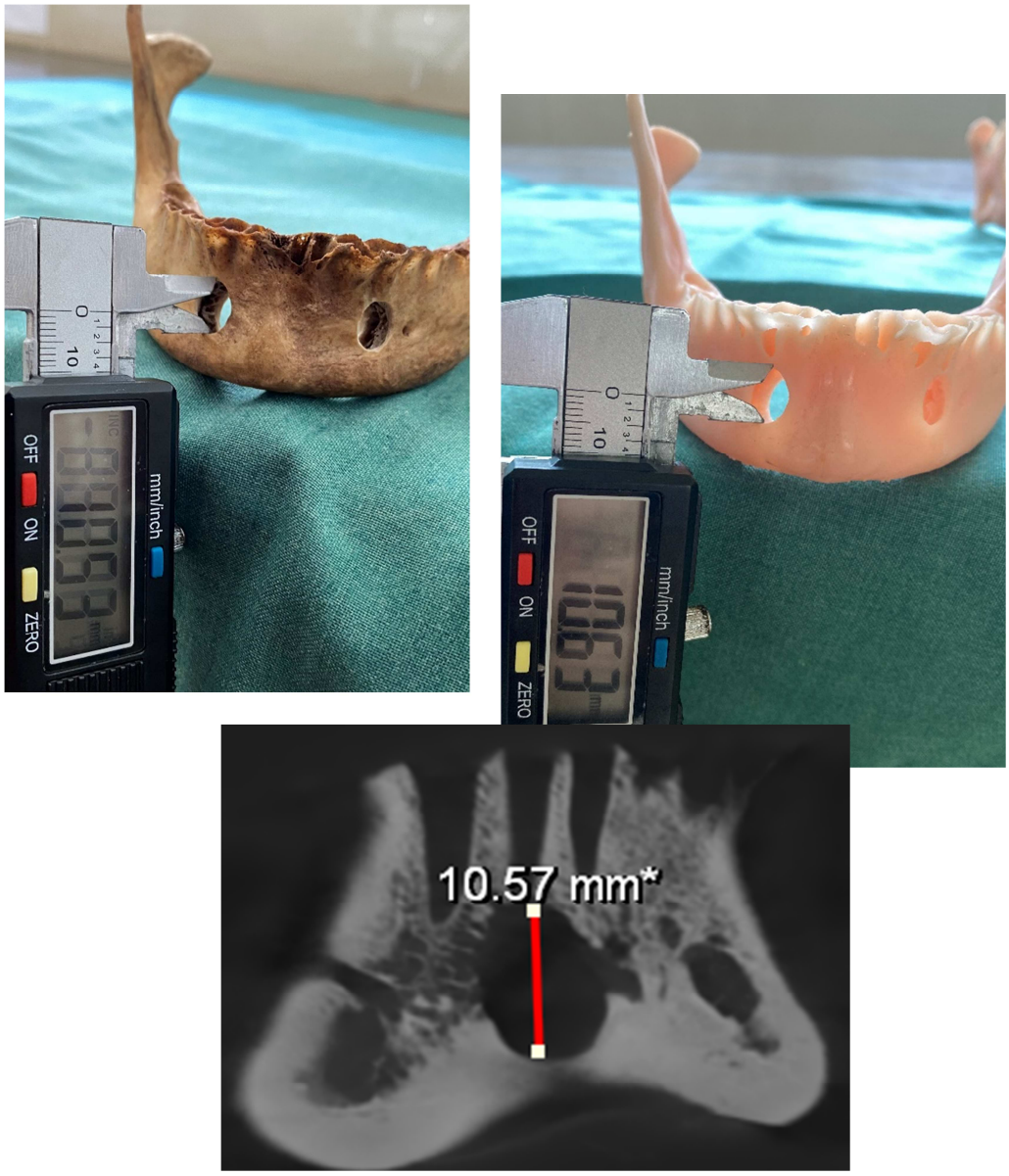

Figure 13: Measurement of circumferential defect height in para symphysis.

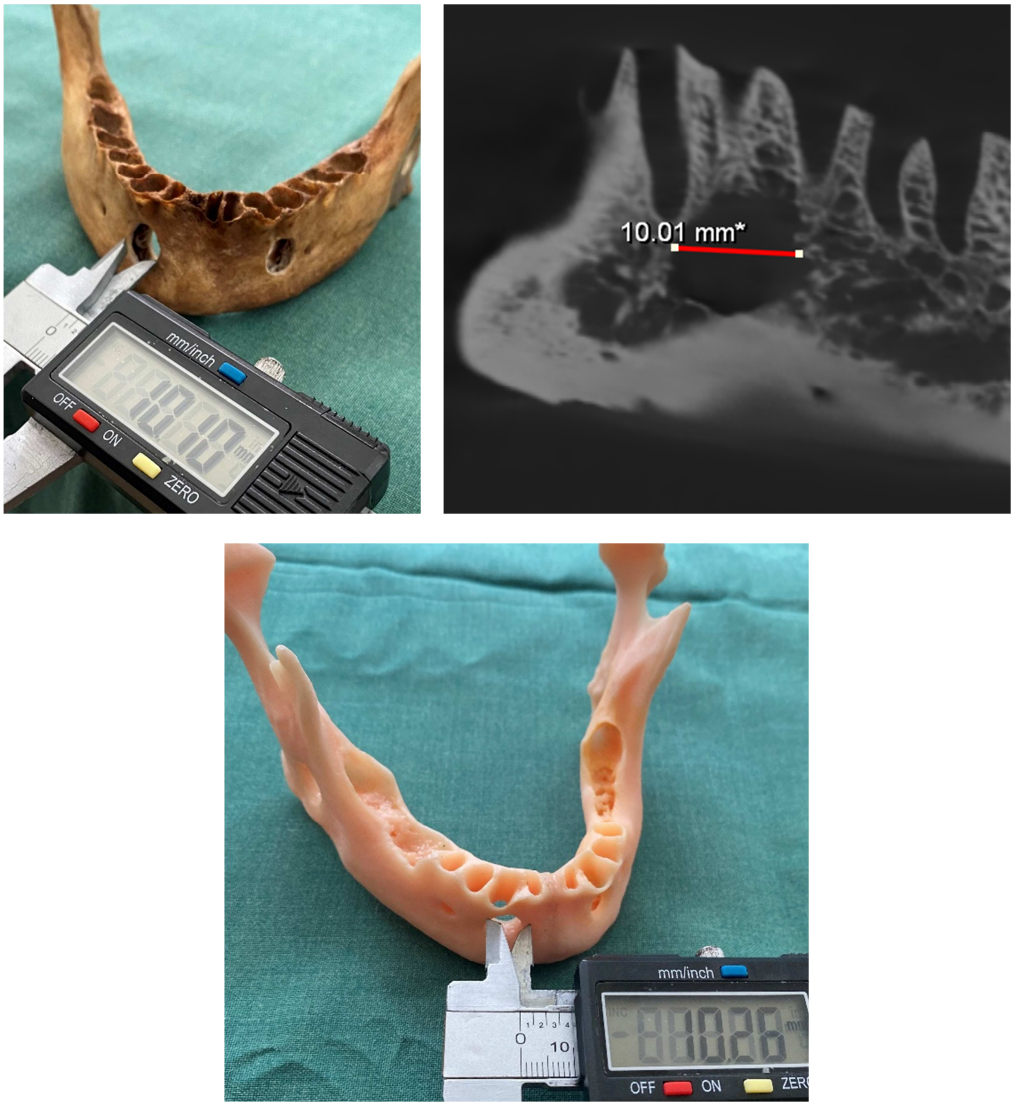

Figure 14: Measurement of circumferential defect width in para symphysis.

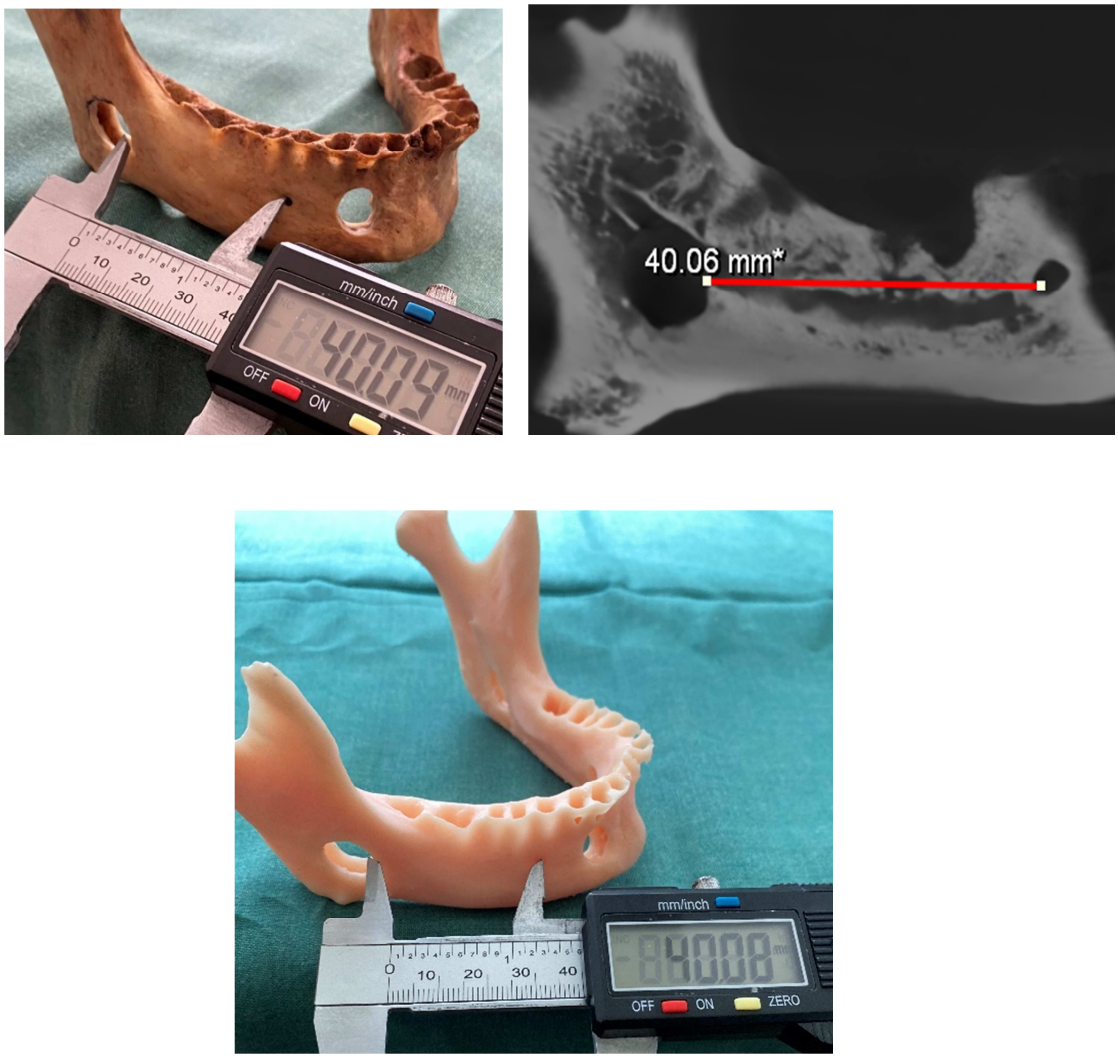

Figure 15: The distance between the circumferential defect in the ramus and mental foramen is measured.

Figure 16: The distance between the circumferential defect in the para symphysis and mental foramen was measured.

RESULTS

In this study, CBCT-scanning and 3D-printing were performed on 10 human dry mandibles. In both the dry mandible measurements and 3D-image, the intra-examiner reproducibility index was 0.90, which is considered high. The ANOVA Tukey's tests were applied at a 5% significance level.

(a) Comparison of circumferential bone defect in ramus between dry mandible, CBCT, and 3D printed model.

Descriptive statistics provided in Table 1, we calculated the mean and standard deviation of all the included parameters. The ANOVA of mean absolute differences in the height of circumferential bone defects on the ramus among dry mandibles, CBCT-images, and 3D-printed models were insignificant ($p = 0.24$) on the right side significant on the left side ($p=0.037$) as shown in Graph 1. In addition, it was noted that the width of the circumferential bone defect on the right side left side of the dry mandible, CBCT scans, and 3D-printed models revealed statistically significant differences as depicted in Graph 2.

The multivariate analysis of the dry mandible, CBCT scans/images, and 3D printed models using a post-hoc Tukey test did not reveal any statistically significant differences ($p > 0.05$) measuring the height of the circumferential defect on the right side as revealed in Table 2. On the left side, the dry mandible and 3D-printed model showed a significant difference ($p =0.033$). Similarly, there was a significant difference ($p = 0.005$ and 0.010) in the width of the circumferential bony defects between dry mandible and 3D-printed models in the right and left ramus.

Table 1: Comparison of the Mean, Standard Deviation variables, and Intergroup variation by one-way ANOVA

		N	Mean	Std. Deviation	Std. Error	Minimum	Maximum	F	Sig.
Right side Height	Dry Mandile	10	10.67	0.03	.00955	10.63	10.72	1.50	0.24
	CBCT	10	10.65	0.03	.01009	10.61	10.71		
	3D Printed Mode	10	10.65	0.03	.00809	10.62	10.70		
Right side Width	Dry Mandile	10	10.33	0.02	.00636	10.30	10.36	6.351	.005*
	CBCT	10	10.31	0.02	.00636	10.28	10.34		
	3D Printed Mode	10	10.30	0.02	.00542	10.28	10.33		
Left side Height	Dry Mandile	10	10.66	0.02	.00667	10.63	10.70	3.75	0.037*
	CBCT	10	10.65	0.02	.00616	10.61	10.68		
	3D Printed Mode	10	10.64	0.02	.00537	10.62	10.67		
Left side Width	Dry Mandile	10	10.33	0.02	.00526	10.31	10.36	5.276	0.012*
	CBCT	10	10.32	0.01	.00423	10.30	10.34		
	3D Printed Mode	10	10.31	0.01	.00379	10.29	10.33		

Table 2: Multiple comparisons of the dry mandible, CBCT, and 3D printed model using Tukey HSD test

Dependent Variable			Mean Difference (I-J)	Std. Error	Sig.	95% Confidence Interval	
						Lower Bound	Upper Bound
Right side Height	Dry Mandile	CBCT	0.02	0.01	.370	-.0145	.0505
		3D Printed Mode	0.02	0.01	.263	-.0115	.0535
	CBCT	Dry Mandile	-0.02	0.01	.370	-.0505	.0145
		3D Printed Mode	0.00	0.01	.972	-.0295	.0355
	3D Printed Mode	Dry Mandile	-0.02	0.01	.263	-.0535	.0115
		CBCT	0.00	0.01	.972	-.0355	.0295
Right side Width	Dry Mandile	CBCT	0.02	0.01	.068	-.0013	.0413
		3D Printed Mode	.03000*	0.01	.005	.0087	.0513
	CBCT	Dry Mandile	-0.02	0.01	.068	-.0413	.0013
		3D Printed Mode	0.01	0.01	.483	-.0113	.0313
	3D Printed Mode	Dry Mandile	-.03000*	0.01	.005	-.0513	-.0087
		CBCT	-0.01	0.01	.483	-.0313	.0113
Left side Height	Dry Mandile	CBCT	0.02	0.01	.171	-.0054	.0374
		3D Printed Mode	.02300*	0.01	.033	.0016	.0444
	CBCT	Dry Mandile	-0.02	0.01	.171	-.0374	.0054
		3D Printed Mode	0.01	0.01	.699	-.0144	.0284
	3D Printed Mode	Dry Mandile	-.02300*	0.01	.033	-.0444	-.0016
		CBCT	-0.01	0.01	.699	-.0284	.0144
Left side Width	Dry Mandile	CBCT	0.01	0.01	.087	-.0017	.0297
		3D Printed Mode	.02000*	0.01	.010	.0043	.0357
	CBCT	Dry Mandile	-0.01	0.01	.087	-.0297	.0017
		3D Printed Mode	0.01	0.01	.614	-.0097	.0217
	3D Printed Mode	Dry Mandile	-.02000*	0.01	.010	-.0357	-.0043
		CBCT	-0.01	0.01	.614	-.0217	.0097

* The difference is significant at the 0.05 level.

Graph 1: Bar chart demonstrating the statistical significance in the Height of circumferential bone defect in the ramus between dry mandible, CBCT, and 3D-printed model

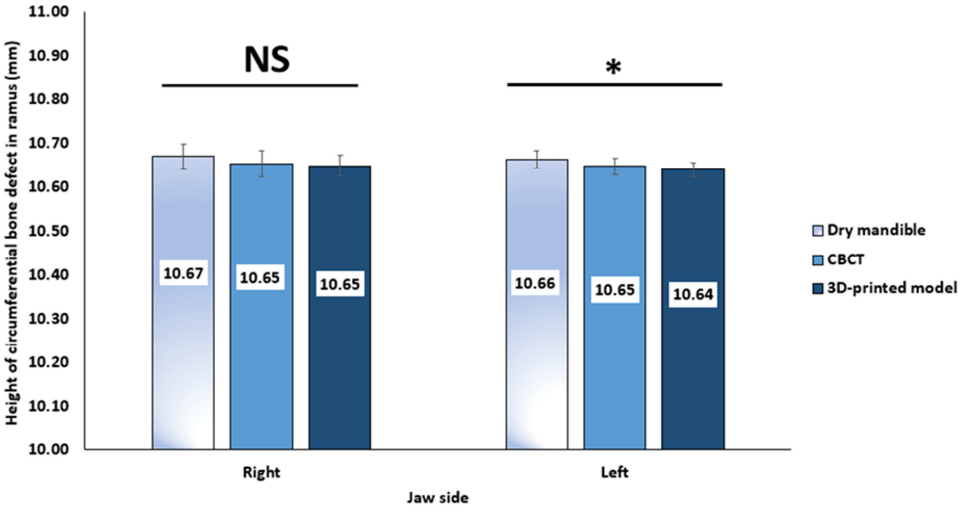

NS- Statistically insignificant, *-Statistically significant

Graph 2: Bar chart demonstrating the statistical significance in the width of circumferential bone defect in ramus between dry mandible, CBCT, and 3D-printed model

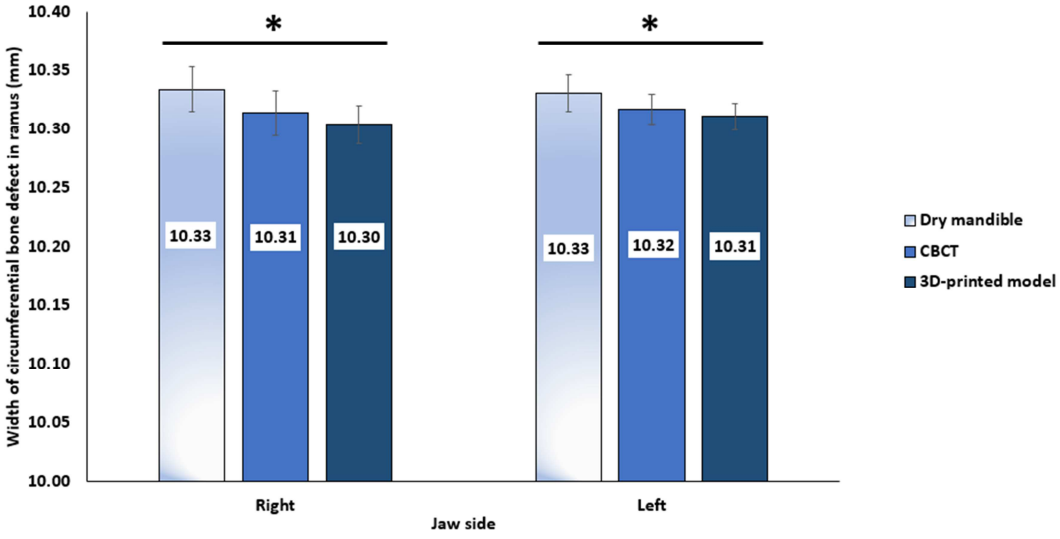

NS- Statistically insignificant, *-Statistically significant

(b) Comparison of circumferential bone defect in Para symphysis between dry mandible, CBCT, and 3D printed model.

Descriptive statistics with mean and standard deviation, for all variables are presented in Table 3. There was a significant difference (p =0.007) in the width of the circumferential defect among dry mandible, CBCT scans/images, and 3D printed model on the right side, whereas there was insignificant difference noted on the left side (p =0.220). Height of the circumferential defect on dry mandible, CBCT scans and 3D-printed models on both right and left was statistically insignificant as shown in Graphs 3 and 4.

The Tukey multiple comparison analysis was performed between the dry mandible, CBCT scans/images, and 3D printed model, as shown in Table 4. The height of the circumferential defect on the right and left Para symphysis revealed no statistical difference. Width on the left side between dry mandible and 3D model revealed no difference, whereas there was a significant difference on right side.

Table 3: Comparison of the Mean, Standard Deviation variables, and Intergroup variation by one-way ANOVA

		N	Mean	Std. Deviation	Std. Error	Minimum	Maximum	F	Sig
Right side Height	Dry Mandile	10	10.6250	.01958	.00619	10.60	10.65	2.818	.077
	CBCT	10	10.6130	.02003	.00633	10.58	10.64		
	3D Printed Mode	10	10.6050	.01716	.00543	10.58	10.63		
Right side Width	Dry Mandile	10	10.3200	.01491	.00471	10.30	10.34	5.975	.007*
	CBCT	10	10.3100	.01491	.00471	10.29	10.33		
	3D Printed Mode	10	10.2970	.01494	.00473	10.27	10.32		
Left side Height	Dry Mandile	10	10.6050	.01716	.00543	10.58	10.63	2.426	.107
	CBCT	10	10.5960	.01647	.00521	10.57	10.62		
	3D Printed Mode	10	10.5880	.01814	.00573	10.56	10.61		
Left side Width	Dry Mandile	10	10.3440	.02221	.00702	10.31	10.38	1.600	.220
	CBCT	10	10.3330	.02163	.00684	10.30	10.37		
	3D Printed Mode	10	10.3260	.02413	.00763	10.29	10.36		

Table 4: Multiple comparisons of dry mandible, CBCT, and 3D printed model using Tukey HSD test

Dependent Variable			Mean Difference (I-J)	Std. Error	Sig.	95% Confidence Interval	
						Lower Bound	Upper Bound
Right side Height	Dry Mandile	CBCT	.01200	.00848	.348	-.0090	.0330
		3D Printed Mode	.02000	.00848	.065	-.0010	.0410
	CBCT	Dry Mandile	-.01200	.00848	.348	-.0330	.0090
		3D Printed Mode	.00800	.00848	.618	-.0130	.0290
	3D Printed Mode	Dry Mandile	-.02000	.00848	.065	-.0410	.0010
		CBCT	-.00800	.00848	.618	-.0290	.0130
Right side Width	Dry Mandile	CBCT	.01000	.00667	.307	-.0065	.0265
		3D Printed Mode	.02300*	.00667	.005	.0065	.0395
	CBCT	Dry Mandile	-.01000	.00667	.307	-.0265	.0065
		3D Printed Mode	.01300	.00667	.145	-.0035	.0295
	3D Printed Mode	Dry Mandile	-.02300*	.00667	.005	-.0395	-.0065
		CBCT	-.01300	.00667	.145	-.0295	.0035
Left side Height	Dry Mandile	CBCT	.00900	.00772	.483	-.0101	.0281
		3D Printed Mode	.01700	.00772	.089	-.0021	.0361
	CBCT	Dry Mandile	-.00900	.00772	.483	-.0281	.0101
		3D Printed Mode	.00800	.00772	.561	-.0111	.0271
	3D Printed Mode	Dry Mandile	-.01700	.00772	.089	-.0361	.0021
		CBCT	-.00800	.00772	.561	-.0271	.0111
Left side Width	Dry Mandile	CBCT	.01100	.01014	.532	-.0141	.0361
		3D Printed Mode	.01800	.01014	.197	-.0071	.0431
	CBCT	Dry Mandile	-.01100	.01014	.532	-.0361	.0141
		3D Printed Mode	.00700	.01014	.771	-.0181	.0321
	3D Printed Mode	Dry Mandile	-.01800	.01014	.197	-.0431	.0071
		CBCT	-.00700	.01014	.771	-.0321	.0181

*. The mean difference is significant at the 0.05 level.

Graph 3: Bar chart demonstrating the statistical significance in the Height of circumferential bone defect in Para symphysis between dry mandible, CBCT, and 3D-printed model

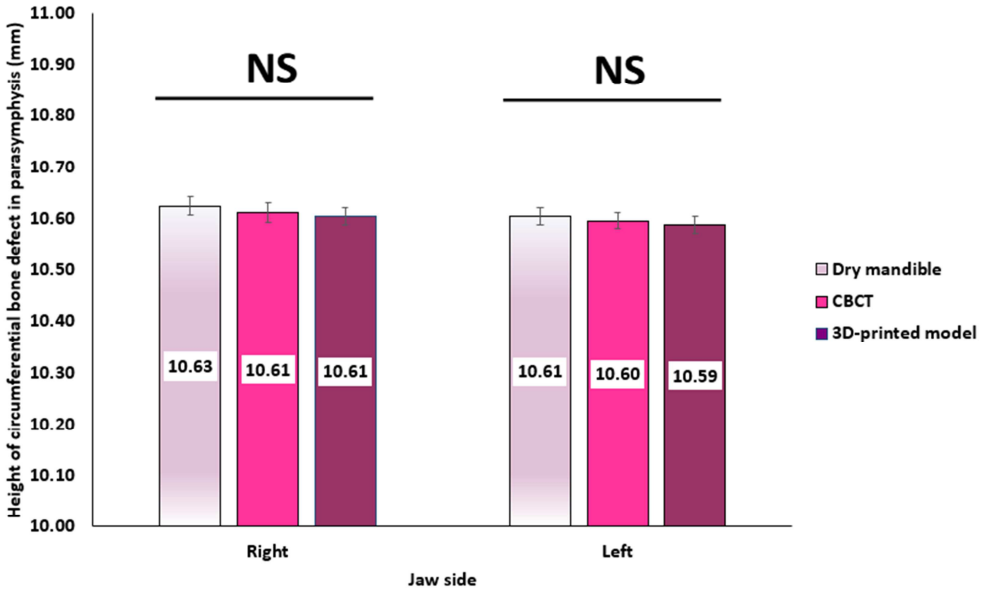

NS- Statistically insignificant, *-Statistically significant

Graph 4: Bar chart demonstrating the statistical significance in the Height of circumferential bone defect in Para symphysis between dry mandible, CBCT, and 3D-printed model

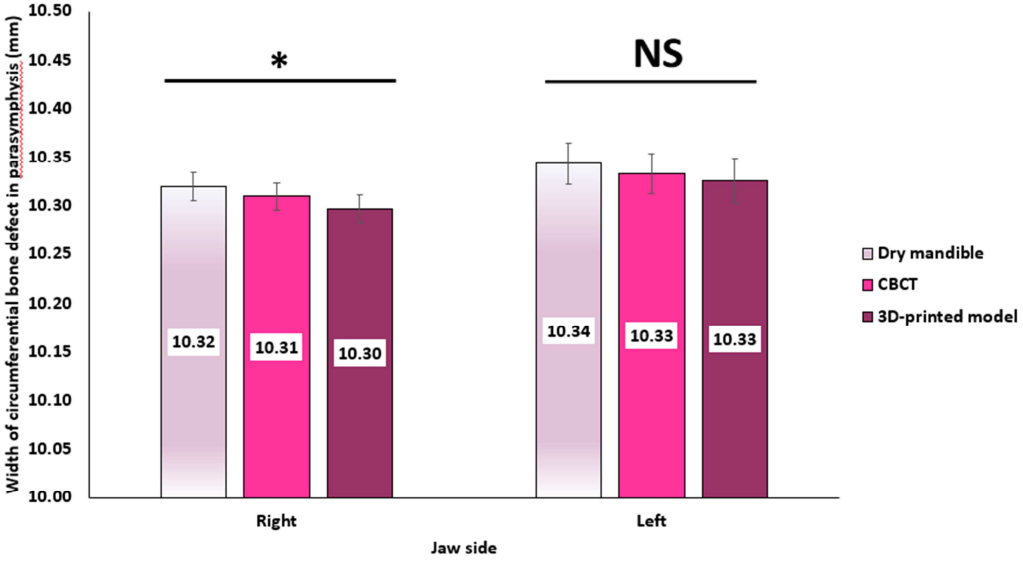

NS- Statistically insignificant, *-Statistically significant

(c) Comparison of length of ramus between dry mandible, CBCT, and 3D-printed model.

According to the descriptive statistics shown in Table 5, the mean measurements of the length of ramus for dry mandibles, CBCT scans and 3D printed models were found to be 5.43, 5.42, and 5.41 on the right side and 5.50, 5.49, 5.48 on the left. Among all the variables, no statistical significance was noted on the right (p=0.94) and left (p=0.96) side, as shown in Graph 5. Tukey multiple comparisons revealed no significant difference between dry mandible, CBCT scans, and 3D printed model in regards to length of the ramus, as noted in Table 6.

Graph 5: Bar chart demonstrating the statistical significance of the Length of ramus between dry mandible, CBCT, and 3D-printed model

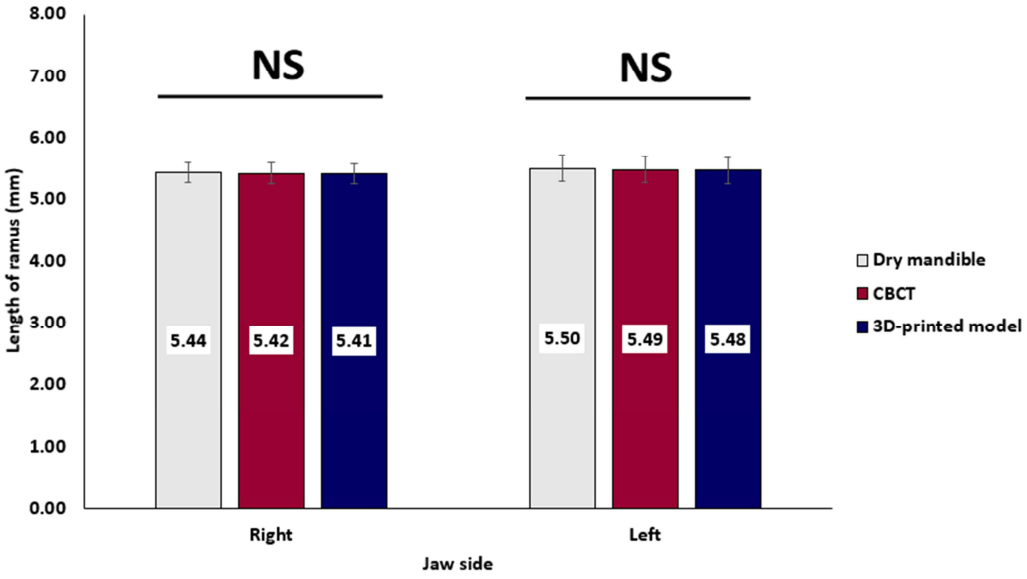

NS- Statistically insignificant, *-Statistically significant

Table 5: Comparison of the Mean, Standard Deviation variables, and Intergroup variation by one-way ANOVA

		N	Mean	Std. Deviation	Std. Error	Minimum	Maximum	F	Sig.
Right side	Dry Mandile	10	4.5250	.19767	.06251	4.22	4.78		
	CBCT	10	4.5150	.19699	.06229	4.21	4.77		
	3D Printed Mode	10	4.5040	.19260	.06090	4.22	4.76	.029	.972
Left side	Dry Mandile	10	4.6040	.27253	.08618	4.16	4.98		
	CBCT	10	4.5940	.27253	.08618	4.15	4.97		
	3D Printed Mode	10	4.5860	.26904	.08508	4.15	4.96	.011	.989

Table 6: Multiple comparisons of dry mandible, CBCT, and 3D printed model using Tukey HSD test

Dependent Variable			**Mean Difference (I-J)**	**Std. Error**	**Sig.**	**95% Confidence Interval**	
						Lower Bound	**Upper Bound**
Right side	Dry Mandile	CBCT	.01500	.07871	.980	-.1802	.2102
		3D Printed Mode	.02600	.07871	.942	-.1692	.2212
	CBCT	Dry Mandile	-.01500	.07871	.980	-.2102	.1802
		3D Printed Mode	.01100	.07871	.989	-.1842	.2062
	3D Printed Mode	Dry Mandile	-.02600	.07871	.942	-.2212	.1692
		CBCT	-.01100	.07871	.989	-.2062	.1842
Left side	Dry Mandile	CBCT	.01500	.10074	.988	-.2348	.2648
		3D Printed Mode	.02500	.10074	.967	-.2248	.2748
	CBCT	Dry Mandile	-.01500	.10074	.988	-.2648	.2348
		3D Printed Mode	.01000	.10074	.995	-.2398	.2598
	3D Printed Mode	Dry Mandile	-.02500	.10074	.967	-.2748	.2248
		CBCT	-.01000	.10074	.995	-.2598	.2398

(d) Comparison of distance from circumferential distance on the ramus to mental foramen between dry mandible, CBCT, and 3D-printed model:

The mean and standard deviation of linear measurements for the circumferential defect in the ramus to mental foramen have been calculated (As indicated in Table 7). Statistically, there is no significant difference noted on the right (p=0.970) and left side (p=0.995) using dry mandible, CBCT scans, and 3D printed models as depicted in Graph 6. In addition to this, the Tukey Post Hoc test revealed no significant difference between all the included variables as shown in Table 8.

Graph 6: Bar chart demonstrating the statistical significance of the distance from circumferential distance on the ramus to mental foramen between dry mandible, CBCT, and 3D-printed model

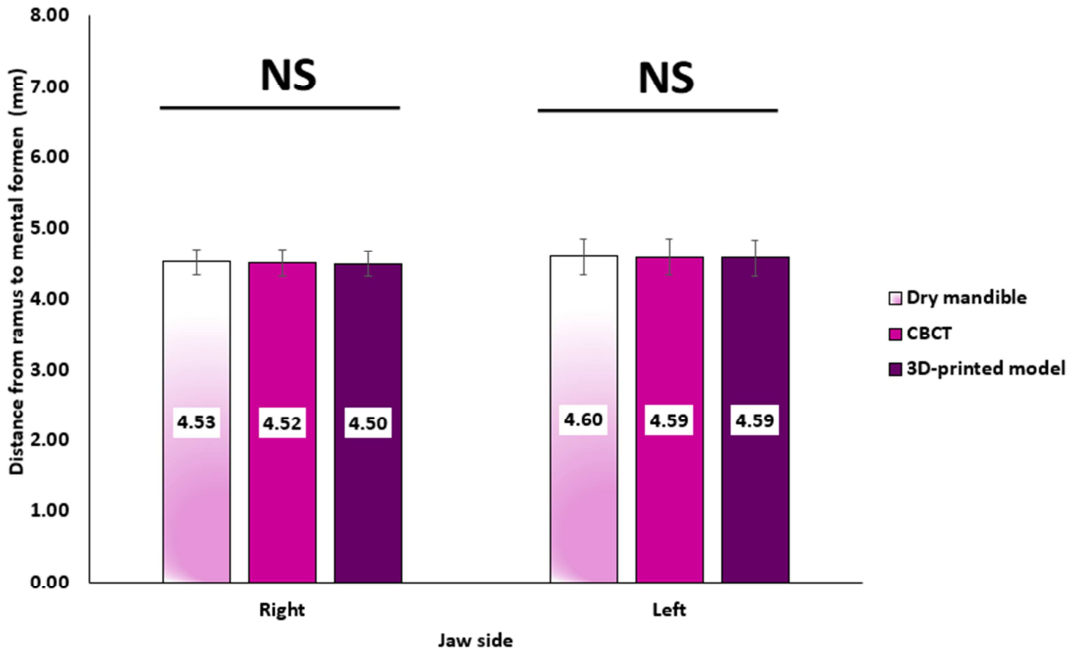

NS- Statistically insignificant, *-Statistically significant

Table 7: Comparison of the Mean, Standard Deviation variables, and Inter group variation by one-way ANOVA

		N	Mean	Std. Deviation	Std. Error	Minimum	Maximum	F	Sig
Right side	Dry Mandile	10	.9660	.17715	.05602	.74	1.22		
	CBCT	10	.9520	.18122	.05731	.72	1.23		
	3D Printed Mode	10	.9470	.17808	.05631	.73	1.22	.030	.970
Left side	Dry Mandile	10	.8820	.21436	.06779	.54	1.21		
	CBCT	10	.8840	.22451	.07100	.53	1.20		
	3D Printed Mode	10	.8750	.22172	.07011	.52	1.19	.005	.995

Table 8: Multiple comparisons of dry mandible, CBCT, and 3D printed model using Tukey HSD test

Dependent Variable			Mean Difference (I-J)	Std. Error	Sig.	95% Confidence Interval	
						Lower Bound	Upper Bound
Right side	Dry Mandile	CBCT	.01400	.07997	.983	-.1843	.2123
		3D Printed Mode	.01900	.07997	.969	-.1793	.2173
	CBCT	Dry Mandile	-.01400	.07997	.983	-.2123	.1843
		3D Printed Mode	.00500	.07997	.998	-.1933	.2033
	3D Printed Mode	Dry Mandile	-.01900	.07997	.969	-.2173	.1793
		CBCT	-.00500	.07997	.998	-.2033	.1933
Left side	Dry Mandile	CBCT	-.00200	.09849	1.000	-.2462	.2422
		3D Printed Mode	.00700	.09849	.997	-.2372	.2512
	CBCT	Dry Mandile	.00200	.09849	1.000	-.2422	.2462
		3D Printed Mode	.00900	.09849	.995	-.2352	.2532
	3D Printed Mode	Dry Mandile	-.00700	.09849	.997	-.2512	.2372
		CBCT	-.00900	.09849	.995	-.2532	.2352

(e) Comparison of distance from circumferential distance on the Para symphysis to mental foramen between dry mandible, CBCT, and 3D-printed model:

The mean and standard deviation of linear measurements of circumferential defect on the Para symphysis to mental foramen have been calculated (As indicated in Table 9). Statistically, there was no significant difference noted on the right (p=0.972) and left side (p=0.989) using dry mandible, CBCT scans and 3D printed models as depicted in Graph 7. In addition to this, the Tukey Post Hoc test revealed no significant difference between all the included variables as shown in Table 10.

Graph 7: Bar chart demonstrating the statistical significance of the circumferential distance from the Para symphysis to mental foramen between dry mandible, CBCT, and 3D-printed model.

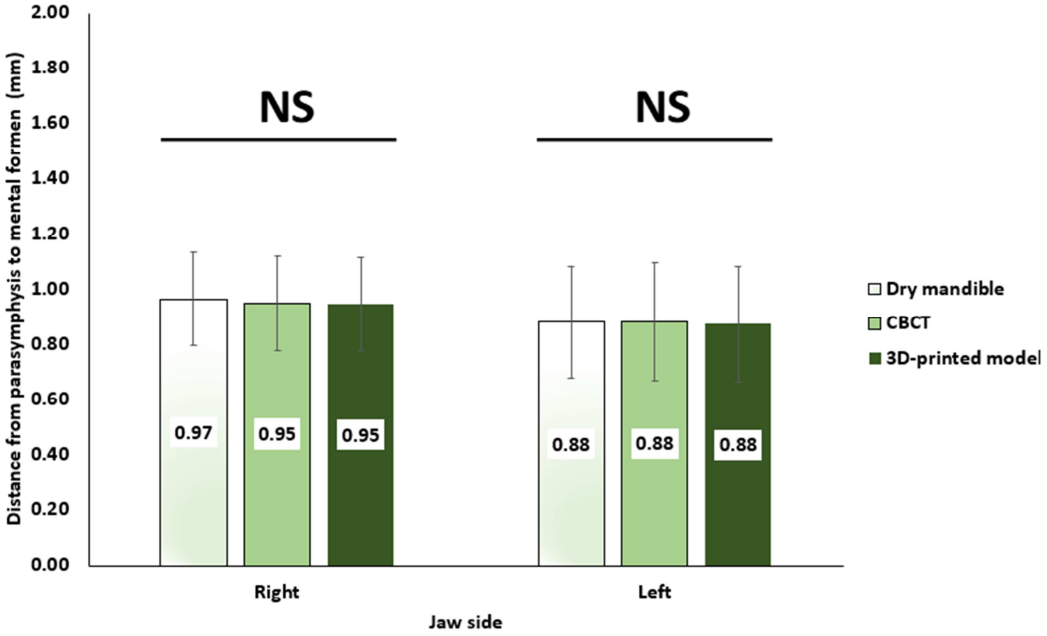

NS- Statistically insignificant, *-Statistically significant

Table 9: Comparison of the Mean, Standard Deviation variables, and Intergroup variation by one-way ANOVA

		N	Mean	Std. Deviation	Std. Error	Minimum	Maximum	F	Sig.
Right side	Dry Mandile	10	4.5250	.19767	.06251	4.22	4.78		
	CBCT	10	4.5150	.19699	.06229	4.21	4.77		
	3D Printed Mode	10	4.5040	.19260	.06090	4.22	4.76	.029	.972
Left side	Dry Mandile	10	4.6040	.27253	.08618	4.16	4.98		
	CBCT	10	4.5940	.27253	.08618	4.15	4.97		
	3D Printed Mode	10	4.5860	.26904	.08508	4.15	4.96	.011	.989

Table 10: Multiple comparisons of dry mandible, CBCT, and 3D printed model using Tukey HSD test

Dependent Variable			Mean Difference (I-J)	Std. Error	Sig.	95% Confidence Interval	
						Lower Bound	Upper Bound
Right side	Dry Mandile	CBCT	.01000	.08755	.993	-.2071	.2271
		3D Printed Mode	.02100	.08755	.969	-.1961	.2381
	CBCT	Dry Mandile	-.01000	.08755	.993	-.2271	.2071
		3D Printed Mode	.01100	.08755	.991	-.2061	.2281
	3D Printed Mode	Dry Mandile	-.02100	.08755	.969	-.2381	.1961
		CBCT	-.01100	.08755	.991	-.2281	.2061
Left side	Dry Mandile	CBCT	.01000	.12136	.996	-.2909	.3109
		3D Printed Mode	.01800	.12136	.988	-.2829	.3189
	CBCT	Dry Mandile	-.01000	.12136	.996	-.3109	.2909
		3D Printed Mode	.00800	.12136	.998	-.2929	.3089
	3D Printed Mode	Dry Mandile	-.01800	.12136	.988	-.3189	.2829
		CBCT	-.00800	.12136	.998	-.3089	.2929

DISCUSSION

In dentistry, radiology plays an integral role in diagnosis, treatment planning, and post-treatment evaluation. Radiographic images are also important diagnostic tools that allow early intervention, preventing the progression of oral diseases and reducing the chances of complications. Further, radiographs provide valuable information about dental problems and act as a guide in decision-making to choose the appropriate treatment option. Radiographic images thus enhance the precision, efficiency, and effectiveness of dental care along with improving outcomes.

Various scientists have contributed to the field of Radiology, among whom Sir C Edmond Kells, is known as the father of dental radiology as he obtained the first intraoral radiograph in 1908, [46]. Following the advent of intraoral radiographs various radiographic techniques were invented which included bitewing radiographs, periapical images of diseased teeth and periodontal issues, and subsequently panoramic radiographs [47]. Interpretation of radiographs is an important skill that is influenced by various factors like a thorough knowledge of the anatomy of the structures in the oro-facial region.

The evolution of Radiology has replaced Conventional film-based imaging with solid-state sensors such as charge-coupled devices, complementary metal oxide semiconductors, and photostimulable phosphor plates [48-49]. The benefits of digital radiography include 90% of dose reduction as compared to E-speed film. Apart from this, it is also possible to measure length, angle, and width in a digital image [50]. However, the only limitation of these images is two-dimensional representations of three-dimensional areas with magnification, distortion, and superimposition [51].

The invention of computed tomography, in 1972, by a British engineer Godfrey Hounsfield and the first dental CT by Schwarz et al [52], helped overcome the limitations of 2D images but the major disadvantages were the high radiation dose, the cost incurred, and the long duration needed for scanning [53].

Later came CBCT which offers several benefits over conventional multi-slice CT scanners. In contrast to CT scanners, CBCT voxels are isotropic and equal in all dimensions. It has a superior image quality to CT due to the high resolution in CBCT [54]. The advantage over CT is that CBCT enables 3D visualization of complex bony structures within the maxillofacial region with very accurate images, high resolution, and is of great diagnostic quality [53]. CBCT is thus becoming the modality of choice for oral health professionals due to its low cost, lower effective radiation dose, and fewer artifacts [54].

3D printing from DICOM pictures is routinely being used in Oral and maxillofacial surgery for patient education, surgical planning and simulation. [55-56]. The development of technology and software, has helped in obtaining 3D models for all patients. This has created new openings and improvised solutions for patient management by integrating CBCT technology with 3D models especially in the field of Oral and Maxillofacial imaging the integration of CBCT and 3D-printing has created new openings and improvised personalized solutions for patient management. Thus treatment planning as well as precise treatment can be customized for every patient improving the outcomes.

In dental practice, the use of CBCT and 3D printed models is increasing, but the accuracy such models must be determined to facilitate their use. As a result, various studies have been conducted to assess the accuracy 3D-printed models.

Nimish et al [57], compared accuracy of linear measurements on human cadaveric mandibles with CBCT images. As per his observation distance measured was greater on mandible was when compared to CBCT images 0.03 ± 0.29 mm.

Similarly, ***Lascala et al*** [58] findings were consistent with the previous studies.

Stratemann et al [59] **studied** CBCT scans of skull and measured linear distances between landmarks for orthodontic analysis and noted differences with New Tom (0.07 ± 0.41) and CB MercuRay (0.00 ± 0.22 mm).

According to ***Joshua et al***., [41], 3D models fabricated with CBCT scans of skull were compared to models derived from an intraoral scanner. The actual width when compared scans revealed 0.5-mm difference in canine whereas 0.44-mm difference in molar.

Zhang et al [60] used CBCT scans of printed 3D anthropomorphic nasal airway model and found a statistically insignificant difference of 0.254. between the readings.

There were consistent findings with a study by ***Mukhia et al*** [61]where in 3D reconstructed models of CBCT images were not significantly different from the reference standard models using 0.2mm or 0.4mm voxels (p=0.50 and 0.16, respectively).

In the present study, human mandibles were compared with CBCT scans and 3D-printed models using several parameters. The results were consistent with the previous studies, thus revealing an insignificant difference (p >0.05) between CBCT images and 3D-printed models while measuring parameters like width of circumferential defects on right and left side ramus was p=0.483 and 0.614, height of circumferential defects on right and left sides of the ramus was (p=0.972 and 0.699). It was also noted that height and width of circumferential defects are not significantly different on right (p=0.618 (h) and

0.145 (W)) and left (p=0.561 (h) and 0.771 (W)) Para symphysis. Furthermore, there were no significant differences in the length on right and left ramus (p=0.989 and 0.995), or the distance from the circumferential defects and mental foramen on either side.

Wang et al [42] examined the accuracy of CBCT-derived skull models fabricated with different technologies. In general, SLA and MJ printed models had significantly lower errors (p=0.01) than FFF printed models, but no additional geometrical differences were observed.

Two CBCT-based surgical simulation techniques were used by ***Chou et al.*** [62] to measure alveolar bone deficiency. Patients with unilateral clefts revealed alveolar defect for virtual-based and 3D printing-based models 1.09 ± 0.24 and 1.09 ± 0.25 mL ($p > 0.05$), whereas patients with bilateral clefts values were 2.05 ± 0.22 and 2.02 ± 0.27 mL ($p > 0.05$). Thus no significant differences were observed with different densities.

Santana et al [13] compared CBCT with 3-dimensional stereolithographic models to identify and measure anterior loop lengths (ANLLs). It was found that CBCT differed insignificantly from anatomic measurements ($p = 0.332$), whereas STL models showed a significant difference from anatomic measurements.

For all the measured parameters in our study, the difference between the dry mandible and the 3D-printed model was insignificant ($p >0.05$). However, the circumferential bony defects on the ramus were significantly different for width on the right and left sides ($p = 0.005$ and 0.010) and for height on the left ($p = 0.033$). Further, there was a significant difference ($p = 0.005$) between mandible and 3D model on the right para-symphysis.

LIMITATIONS:

The dimensional accuracy of the 3D printed models can be affected by variations in CBCT machines, 3D printing methods, and materials. In the current study, the data was acquired using the same image acquisition protocol with one CBCT machine. Hence to assess reproducibility, other 3D printing methods and materials should have been used.

The SLA method of 3D printing with resin is very precise and provides excellent detail, but manufacturing time and costs are the main limitations of using this printing technique.

A digital vernier callipers was used in the current study for measurements on the human dry mandibles and 3D-printed models. Using this manual technique can lead to multiple errors due to, Operator bias, and errors in landmark identification.

Cylindrical plastic has been used to simulate the soft tissues of dry mandibles, however, the soft tissues of live patients and other factors associated with the intraoral environment may affect the accuracy of the imaging by scattering radiation, affecting gray level value differentiation, and lowering bone image quality.

FUTURE PROSPECTS OF THE STUDY

1. To determine the geometric accuracy of CBCT 3D models and observe their clinical outcomes.
2. To validate the entire computerized workflow.
3. Future studies need to focus on determining the reproducibility and accuracy of different softwares which vary with CBCT scanners and image acquisition protocols.
4. Further studies should be conducted to test cytotoxicity and sterilization to ensure that 3D-printed models are safe to use in the operating room.

5. A complex anatomical structure such as the entire skull needs to be scanned, to assess the reproducibility of the 3D models based on CBCT scans.

SUMMARY AND CONCLUSION

Advent of CBCT and 3D printing has revolutionized various fields, particularly the healthcare sector. This technology allows us to transform digital data acquired from CBCT scans into exact replica of the object with 3D printing. The purpose of the present study was to assess accuracy of measurements obtained on dry mandible, CBCT scans and 3D models, so as to advocate their use in clinical practice.

A total of 14 linear measurements were made on anatomical landmarks and artificially created defects on dry mandibles and were measured on mandibles, CBCT scans and 3D-printed models. Among all variables only 4 parameters revealed some differences in measurements. This proves that all the variables can be used reliably for various clinical applications in Dentistry.

Thus, this study concludes that the applications of CBCT and 3D-printed models go way beyond diagnosis, treatment planning, and intervention. It was found that there was a slight variation in the measurements from dry mandibles, CBCT images and models. Thus, all the variables can be used for a variety of clinical applications in dentistry like accurately diagnosing maxillofacial pathologies and planning treatment for these pathologies as well as implant planning, etc. The findings of the study has endorsed accuracy of 3D models and CBCT scans for potential practical implications in dentistry.

KEYNOTE

1) CBCT scans provide the key data needed to perform medical 3D printing, enabling the fabrication of highly precise and personalized models.
2) It was observed that there was a no difference between the dry mandibles and their CBCT images, with the parameters measured.

3) As a result of CBCT and 3D printing, all parameters were measured similarly without any differences.

4) Variations were noted with few parameters in 3D printed models and dry mandibles.

BIBLIOGRAPHY

1. Friedland B. Medicolegal issues related to cone beam CT. InSeminars in Orthodontics 2009 Mar 1 (Vol. 15, No. 1, pp. 77-84). WB Saunders.

2. Shweel M, Amer MI, El-shamanhory AF. A comparative study of cone-beam CT and multidetector CT in the preoperative assessment of odontogenic cysts and tumors. The Egyptian Journal of Radiology and Nuclear Medicine. 2013 Mar 1;44(1):23-32.

3. Weber AL. History of head and neck radiology: past, present and future. Radiol 2001;218:15-24.

4. Venkatesh E, Elluru SV. Cone beam computed tomography: basics and applications in dentistry. J Istanb Univ Fac Dent. 2017 Dec 2;51(3 Suppl 1):S102-S121

5. Ludlow JB, Gubler M, Cevidanes L, Mol A. Precision of cephalometric landmark identification: cone-beam computed tomography vs conventional cephalometric views. American Journal of Orthodontics and Dentofacial Orthopedics. 2009 Sep 1;136(3):312-e1.

6. Bayome M, Park JH, Kim Y, Kook YA. 3D analysis and clinical applications of CBCT images. InSeminars in Orthodontics 2015 Dec 1 (Vol. 21, No. 4, pp. 254-262). WB Saunders.

7. Macleod I, Heath N. Cone-beam computed tomography (CBCT) in dental practice. Dental update. 2008 Nov 2;35(9):590-8.

8. Katheria BC, Kau CH, Tate R, Chen JW, English J, Bouquot J. Effectiveness of impacted and supernumerary tooth diagnosis from traditional radiography versus cone beam computed tomography. Pediatr Dent. 2010 Jul-Aug;32(4):304-9.

9. Alsufyani NA, Flores-Mir C, Major PW. Three-dimensional segmentation of the upper airway using cone beam CT: a systematic review. Dentomaxillofac Radiol. 2012 May;41(4):276-84

10. Bayome M, Park JH, Kook YA. New three-dimensional cephalometric analyses among adults with a skeletal Class I pattern and normal occlusion. Korean J Orthod. 2013 Apr;43(2):62-73. doi: 10.4041/kjod.2013.43.2.62. Epub 2013 Apr 25.

11. Dawood A, Marti BM, Sauret-Jackson V, Darwood A. 3D printing in dentistry. British dental journal. 2015 Dec;219(11):521-9.

12. Grant GT (2015) Direct Digital Manufacturing. In: Masri R, Driscoll CF (eds) Clinical applications of digital dental technology, 1st edn. Wiley-Blackwell, Oxford, pp 41–55

13. Santana RR, Lozada J, Kleinman A, Al-Ardah A, Herford A, Chen JW. Accuracy of cone beam computerized tomography and a three-dimensional stereolithographic model in identifying the anterior loop of the mental nerve: a study on cadavers. J Oral Implantol. 2012 Dec;38(6):668-76.

14. Pandey M, Choudhury H, Fern JLC, Kee ATK, Kou J, Jing JLJ, et al. 3D printing for oral drug delivery: a new tool to customize drug delivery. Drug Deliv Transl Res. 2020;10(4):986–1001.

15. Oberoi, G.; Nitsch, S.; Edelmayer, M.; Janji´c, K.; Müller, A.S.; Agis, H. 3D Printing—Encompassing the Facets of Dentistry. Front. Bioeng. Biotechnol. 2018, 6, 172

16. Barazanchi A, Li KC, Al-Amleh B, Lyons K, Waddell JN. Additive Technology: Update on Current Materials and Applications in Dentistry. J Prosthodont. 2017 Feb;26(2):156-163.

17. Textbook of Dental Radiology- Pramod John R second edition

18. Essentials of Dental Radiography and Radiology- Eric whaites Third edition

19. AAOMR at https://www.aaomr.org/assets/History/early_pioneers_of_oral_and_m.pdf

20. Lohia S, Joshi AS. Idiopathic sialectasis of the Stensen's duct treated with marsupialisation. BMJ Case Rep. 2013 Nov 14;2013:bcr2013201548.

21. Tammisalo EH. Professor yrjö v. Paatero - the pioneer of panoramic oral tomography. Dentomaxillofac Radiol. 1975 Jan;4(1):53-6.

22. Yoshida M, Yoshihara H, Honda E (2018) History of Digital Detectors in Intraoral Radiography. Dent Health Curr Res 4:2.

23. Borg E. Some characteristics of solid-state and photo-stimulable phosphor detectors for intra-oral radiography. Swed Dent J Suppl. 1999;139:i-viii, 1-67.

24. L. W. Goldman, “Principles of CT and the evolution of CT technology,” in Categorical Course in Diagnostic Radiology Physics: CT and US Cross sectional Imaging, L. W. Goldman and J. B. Fowlkes, Eds., Radiological Society of North America, Inc., Oak Brook, IL (2000).

25. Parks ET, Williamson GF. Digital radiography: an overview. J Contemp Dent Pract. 2002 Nov 15;3(4):23-39.

26. Tam KC, Samarasekera S, Sauer F. Exact cone beam CT with a spiral scan. Phys Med Biol. 1998 Apr;43(4):1015-24

27. Mah J, Hatcher D. Current status and future needs in craniofacial imaging. Orthod Craniofac Res. 2003;6 Suppl 1:10-6; discussion 179-82.

28. Cone Beam CT of the Head and Neck- An Anatomical Atlas

29. ASTM F2792-12a, “Standard Terminology for Additive Manufacturing Technologies,” (Withdrawn 2015) ASTM International, pp. 1–3, West Conshohocken, PA, 2012.

30. First commercialised of the 3D printing processes in year 1980 by Charles Hull.

31. Derby B. Additive manufacture of ceramics components by inkjet printing. Engineering. 2015 Mar 1;1(1):113-23.

32. Kamburoğlu K, Kolsuz E, Kurt H, Kılıç C, Özen T, Semra Paksoy C. Accuracy of CBCT measurements of a human skull. Journal of digital imaging. 2011 Oct;24:787-93.

33. Menezes CC, Janson G, da Silveira Massaro C, Cambiaghi L, Garib DG. Precision, reproducibility, and accuracy of bone crest level measurements of CBCT cross sections using different resolutions. The Angle Orthodontist. 2016 Jul;86(4):535-42.

34. Fernandes TM, Adamczyk J, Poleti ML, Henriques JF, Friedland B, Garib DG. Comparison between 3D volumetric rendering and multiplanar slices on the reliability of linear measurements on CBCT images: an in vitro study. Journal of Applied Oral Science. 2014 Jul 4;23:56-63.

35. Jung H, Kim HJ, Kim DO, Hong SI, Jeong HK, Kim KD, Kim Y, Yoo S, Yoo H. Quantitative analysis of three-dimensional rendered imaging of the human skull acquired from multi-detector row computed tomography. Journal of Digital Imaging. 2002 Dec;15(4):232.

36. Loubele M, Guerrero ME, Jacobs R, Suetens P, Van Steenberghe D. A comparison of jaw dimensional and quality assessments of bone characteristics with cone-beam CT, spiral tomography, and multi-slice spiral CT. International Journal of Oral & Maxillofacial Implants. 2007 May 1;22(3).

37. Silva AA, Franco A, Fernandes Â, Costa C, Barbosa JS, Westphalen FH. Accuracy of linear measurements performed with two imaging software in cone-beam computed tomography scans of dry human mandibles. Anais da Academia Brasileira de Ciências. 2017 Dec 7;89:2865-73.

38. Olszewski R, Szymor P, Kozakiewicz M. Accuracy of three-dimensional, paper-based models generated using a low-cost, three-dimensional printer. J Craniomaxillofac Surg. 2014 Dec;42(8):1847-52Almeida VSM, Bomfim RT, Sobreira ACR, Barbosa IDS, Leite-Ribeiro PM, Rubira-Bullen IR, Sarmento VA. Linear measurement accuracy of CBCT panoramic reconstructions: experimental study with dry human mandibles. Oral Radiol. 2021 Jul;37(3):421-426.

39. Santana RR, Lozada J, Kleinman A, Al-Ardah A, Herford A, Chen JW. Accuracy of cone beam computerized tomography and a three-dimensional stereolithographic model in identifying the anterior loop of the mental nerve: a study on cadavers. J Oral Implantol. 2012 Dec;38(6):668-76.

40. Poleti ML, Fernandes TMF, Moretti MR, Puzinato LR, Slaviero TVS, Rubira-Bullen IRF. Reliability and accuracy of automatic segmentation of mandibular 3D models on linear measurements. Clin Oral Investig. 2021 Nov;25(11):6335-6346.

41. Ferraro JM, Falter J, Lee S, Watanabe K, Wu TH, Kim DG, Ko CC, Tanaka E, Deguchi T. Accuracy of three-dimensional printed models derived from cone-beam computed tomography. The Angle Orthodontist. 2022 Nov 1;92(6):722-7.

42. Wang X, Shujaat S, Shaheen E, Ferraris E, Jacobs R. Trueness of cone-beam computed tomography-derived skull models fabricated by different technology-based three-dimensional printers. BMC Oral Health. 2023 Dec;23(1):1-9.

43. Ibrahim D, Broilo TL, Heitz C, de Oliveira MG, de Oliveira HW, Nobre SM, dos Santos Filho JH, Silva DN. Dimensional error of selective laser sintering, three-dimensional printing and PolyJet™ models in the reproduction of mandibular anatomy. Journal of Cranio-Maxillofacial Surgery. 2009 Apr 1;37(3):167-73.

44. Yousefi F, Shokri A, Farhadian M, Vafaei F, Forutan F. Accuracy of maxillofacial prototypes fabricated by different 3-dimensional printing technologies using multi-slice and cone-beam computed tomography. Imaging Sci Dent. 2021 Mar;51(1):41-47

45. Primo BT, Presotto AC, de Oliveira HW, Gassen HT, Miguens SA Jr, Silva AN Jr, Hernandez PA. Accuracy assessment of prototypes produced using multi-slice and cone-beam computed tomography. Int J Oral Maxillofac Surg. 2012 Oct;41(10):1291-5

46. Jacobsohn PH, Fedran RJ. Making darkness visible: the discovery of X-ray and its introduction to dentistry. The Journal of the American Dental Association. 1995 Oct 1;126(10):1359-66.

47. Persson RE, Tzannetou S, Feloutzis AG, Brägger U, Persson GR, Lang NP. Comparison between panoramic and intra-oral radiographs for the assessment of alveolar bone levels in a periodontal maintenance population. Journal of clinical periodontology. 2003 Sep;30(9):833-9.

48. Todd R. Dental imaging—2 D to 3 D: a historic, current, and future view of projection radiography. Endodontic Topics. 2014 Nov;31(1):36-52.

49. Van Der Stelt PF. Filmless imaging: the uses of digital radiography in dental practice. The Journal of the American Dental Association. 2005 Oct 1;136(10):1379-87.

50. Jayachandran S. Digital Imaging in Dentistry: A Review. Contemp Clin Dent. 2017 Apr-Jun;8(2):193-194.

51. American Dental Association Council on Scientific Affairs. The use of dental radiographs: update and recommendations. The Journal of the American Dental Association. 2006 Sep 1;137(9):1304-12.

52. Schwarz MS, Rothman SL, Rhodes ML, Chafetz N. Computed tomography: Part I. Preoperative assessment of the mandible for endosseous implant surgery. International Journal of Oral & Maxillofacial Implants. 1987 Jun 1;2(3).

53. Sethi P, Tiwari R, Das M, Singh MP, Agarwal M, Ravikumar AJ. Two dimensional versus three-dimensional imaging in endodontics—an updated. system. 2016;10:11.

54. Holberg C, Steinhäuser S, Geis P, Rudzki-Janson I. Cone-beam computed tomography in orthodontics: benefits and limitations. Journal of orofacial orthopedics= Fortschritte der Kieferorthopadie: Organ/official journal Deutsche Gesellschaft fur Kieferorthopadie. 2005 Nov 1;66(6):434-44.

55. Kikano E, Grosse Hokamp N, Ciancibello L, Ramaiya N, Kosmas C, Gupta A. Utility of virtual monoenergetic images from spectral detector computed tomography in improving image segmentation for purposes of 3D printing and modeling. 3D Printing in Medicine. 2019 Dec;5(1):1-8.

56. Flores RL, Liss H, Raffaelli S, Humayun A, Khouri KS, Coelho PG, Witek L. The technique for 3D printing patient-specific models for auricular reconstruction. Journal of Cranio-Maxillofacial Surgery. 2017 Jun 1;45(6):937-43.

57. Karjodkar F, Sansare K, Prakash N, Arora AS, Arwade R. Assessment of the Accuracy of Linear Measurements on Human Mandible using Cone Beam Computed Tomography. Journal of Contemporary Dentistry. 2017 Jul 1;8(1):14-9.

58. Lascala CA, Panella J, Marques MM. Analysis of the accuracy of linear measurements obtained by cone beam computed tomography (CBCT-NewTom). Dentomaxillofacial Radiology. 2004 Sep;33(5):291-4.

59. Stratemann SA, Huang JC, Maki K, Miller AJ, Hatcher DC. Comparison of cone beam computed tomography imaging with physical measures. Dentomaxillofacial Radiology. 2008 Feb;37(2):80-93.

60. Zhang C, Bruggink R, Baan F, Bronkhorst E, Maal T, He H, Ongkosuwito EM. A new segmentation algorithm for measuring CBCT images of nasal airway: a pilot study. PeerJ. 2019 Jan 28;7:e6246.

61. Mukhia N, Birur NP, Shubhasini AR, Shubha G, Keerthi G. Dimensional measurement accuracy of 3-dimensional models from cone beam computed tomography using different voxel sizes. Oral Surgery, Oral Medicine, Oral Pathology and Oral Radiology. 2021 Sep 1;132(3):361-9.

62. Chou PY, Denadai R, Hallac RR, Dumrongwongsiri S, Hsieh WC, Pai BC, Lo LJ. Comparative volume analysis of alveolar defects by 3D simulation. Journal of clinical medicine. 2019 Sep 6;8(9):1401.

ANNEXURE – I

ETHICAL CLEARANCE CERTIFICATE

Research and Ethics Committee
KLE VK INSTITUTE OF DENTAL SCIENCES
A Constituent Unit of KLE Academy of Higher Education & Research
Accredited 'A' Grade by NAAC Placed in Category 'A' by MHRD (GoI)
Nehru Nagar, Belagavi - 590 010, Karnataka State
☎: 0831-2470362 Web: http://www.kledental-bgm.edu.in
FAX: 0831-2470640 E-mail:principal@kledental-bgm.edu.in

Sl. No. : 1571

CERTIFICATE

EC/NEW/INST/2021/2435
Research & Ethics Committee

This is to Certify that the synopsis titled

Evaluating and Comparing bony defects on human dry mandibles with CBCT images and 3D printed model. - An vitro study

Submitted by

Reg no: IG0221001

from Department of

Oral Medicine and Radiology *has been critically evaluated by committee members and granted ethical clearance to conduct the above mentioned study*

Date : 11/3/24

Member Secretary
Research and Ethical Committee
KLEVK Institute of Dental Sciences
Belagavi

MEMBER SECRETARY
Research & Ethical Committee
KLEVK Institute of Dental Sciences
BELAGAVI.

Chairman
Research and Ethical Committee
KLEVK Institute of Dental Sciences
Belagavi

Annexure-II: MASTER CHART- Circumferential bone defect on right and left ramus

S.no	Circumferential bone defect- Ramus						Circumferential bone defect- Ramus					
	Right side- Height			Left side- Height			Right side- Width			Left side- Width		
	Dry mandible	CBCT	3D-printed model	Dry mandible	CBCT	3D-printed model	Dry mandible	CBCT	3D-printed model	Dry mandible	CBCT	3D-printed model
1	10.65	10.63	10.64	10.63	10.61	10.62	10.33	10.32	10.31	10.32	10.31	10.31
2	10.65	10.64	10.63	10.66	10.65	10.64	10.32	10.3	10.3	10.31	10.31	10.3
3	10.68	10.65	10.66	10.67	10.65	10.64	10.34	10.31	10.3	10.33	10.33	10.32
4	10.7	10.68	10.67	10.65	10.63	10.62	10.3	10.28	10.28	10.31	10.3	10.29
5	10.65	10.62	10.63	10.69	10.66	10.67	10.35	10.33	10.31	10.34	10.32	10.31
6	10.72	10.71	10.7	10.7	10.68	10.66	10.34	10.32	10.3	10.36	10.34	10.33
7	10.63	10.61	10.62	10.66	10.65	10.64	10.36	10.34	10.33	10.35	10.33	10.32
8	10.64	10.63	10.62	10.64	10.63	10.62	10.36	10.34	10.33	10.32	10.3	10.31
9	10.68	10.67	10.66	10.67	10.66	10.64	10.33	10.31	10.3	10.34	10.32	10.32
10	10.7	10.68	10.66	10.66	10.65	10.65	10.31	10.29	10.28	10.33	10.31	10.3

Annexure-III: MASTER CHART- Circumferential bone defect on right and left parasymphysis

S.no	Circumferential bone defect- Parasymphysis						Circumferential bone defect- Parasymphysis					
	Right side- Height			Left side- Height			Right side- Width			Left side- Width		
	Dry mandible	CBCT	3D-printed model	Dry mandible	CBCT	3D-printed model	Dry mandible	CBCT	3D-printed model	Dry mandible	CBCT	3D-printed model
1	10.6	10.58	10.59	10.62	10.61	10.6	10.31	10.3	10.29	10.36	10.34	10.34
2	10.62	10.61	10.6	10.59	10.59	10.58	10.3	10.29	10.29	10.34	10.33	10.32
3	10.65	10.63	10.62	10.62	10.61	10.6	10.34	10.33	10.32	10.38	10.37	10.36
4	10.63	10.62	10.61	10.63	10.62	10.61	10.33	10.32	10.3	10.37	10.36	10.36
5	10.6	10.59	10.58	10.59	10.58	10.57	10.32	10.31	10.3	10.35	10.34	10.34
6	10.61	10.6	10.59	10.58	10.57	10.56	10.31	10.3	10.28	10.33	10.32	10.31
7	10.65	10.64	10.63	10.61	10.6	10.6	10.3	10.29	10.27	10.32	10.31	10.3
8	10.64	10.63	10.62	10.62	10.61	10.61	10.34	10.33	10.31	10.31	10.3	10.29
9	10.61	10.6	10.59	10.6	10.59	10.58	10.33	10.32	10.31	10.33	10.32	10.31
10	10.64	10.63	10.62	10.59	10.58	10.57	10.32	10.31	10.3	10.35	10.34	10.33

Annexure-IV: MASTER CHART-length of ramus

S.no	Length of Ramus					
	Right side			Left side		
	Dry mandible	CBCT	3D-printed model	Dry mandible	CBCT	3D-printed model
1	5.18	5.17	5.16	5.61	5.59	5.58
2	5.52	5.53	5.52	5.43	5.43	5.42
3	5.58	5.57	5.56	5.42	5.4	5.39
4	5.56	5.5	5.49	5.23	5.21	5.22
5	5.31	5.29	5.28	5.39	5.38	5.37
6	5.55	5.54	5.53	5.23	5.21	5.2
7	5.48	5.47	5.47	5.36	5.34	5.33
8	5.18	5.17	5.17	5.78	5.77	5.75
9	5.34	5.32	5.28	5.67	5.66	5.64
10	5.69	5.68	5.67	5.89	5.87	5.86

Annexure-V: MASTER CHART- Distance between circumferential bone defect from parasymphysis to mental foramen

S.no	Circumferential defect (Parasymphysis)- Mental foramen					
	Right side			Left side		
	Dry mandible	CBCT	3D-printed model	Dry mandible	CBCT	3D-printed model
1	0.74	0.72	0.73	0.63	0.62	0.63
2	1.13	1.12	1.11	0.54	0.53	0.52
3	1.22	1.23	1.22	1.21	1.2	1.19
4	0.79	0.78	0.78	0.77	0.77	0.76
5	0.84	0.84	0.83	0.88	0.87	0.86
6	1.22	1.2	1.19	1.18	1.17	1.16
7	0.99	0.97	0.96	0.95	0.94	0.92
8	0.87	0.84	0.83	0.82	0.81	0.8
9	1.02	1	1.01	1	1.11	1.1
10	0.84	0.82	0.81	0.84	0.82	0.81

Annexure-VI: MASTER CHART- Distance between circumferential bone defect on ramus to Mental foramen

S.no	Circumferential defect (Ramus)- Mental foramen					
	Right side			Left side		
	Dry mandible	CBCT	3D-printed model	Dry mandible	CBCT	3D-printed model
1	4.22	4.21	4.22	4.18	4.17	4.17
2	4.54	4.53	4.53	4.16	4.15	4.15
3	4.42	4.41	4.4	4.98	4.97	4.96
4	4.32	4.31	4.3	4.86	4.85	4.84
5	4.57	4.56	4.54	4.52	4.51	4.5
6	4.65	4.65	4.63	4.62	4.61	4.61
7	4.32	4.31	4.29	4.53	4.52	4.51
8	4.78	4.76	4.74	4.73	4.72	4.71
9	4.65	4.64	4.63	4.62	4.61	4.59
10	4.78	4.77	4.76	4.84	4.83	4.82